# Exergoeconomic Analysis and Comparison Between Ammonia/Water and Ammonia/Salt Solar Absorption Refrigeration Cycles

**Reyhaneh Rabiei[1], Mehdi Borji[2*],Admin Kazemi[3]**

**Abstract**–This research analyzes and compares the exergy and exergoeconomic performance of six chiller configurations to produce 300 Kw of cooling. The configurations are the simple absorption and the combined ejector-absorption refrigeration cycles using ammonia-water ($NH_3$-$H_2O$), ammonia-lithium nitrate ($NH_3$-$LiNO_3$) and ammonia-sodium thiocyanate ($NH_3$-NaSCN) driven by flat plate solar collector and storage tank. The objective of this research is to determine which ammonia-based working fluids provide superior performance in solar absorption cooling systems. The results show that with an increase of the generator temperature in the absorption cycles, as well as with an increase of the ejector pressure ratio in the combined ejector-absorption cycle with $NH_3$-NaSCN as working fluid, the solar and economic factors improve, especially at higher generator temperatures compared to these cycles with $NH_3$-$LiNO_3$ and $NH_3$-$H_2O$ as working fluids. Regarding the unit cost of cooling production, the studied cycles with $NH_3$-$LiNO_3$ show a better performance. In the combined ejector cycle with ammonia-sodium thiocyanate, which has the best performance among the cycles studied, the solar coefficient of performance and the solar exergy efficiency are equal to 0.21 and 1.659%, respectively. Also, the total cost rate and the unit cost of cooling production in the mentioned cycle are equal to 415.7 $\frac{\$}{hr}$and 52.15 $\frac{\$}{GJ}$, respectively.

**Keywords**: Exergoeconomic analysis, Absorption cycle, Solar collector, Ammonia-water, Ammonia-salt

## 1. Introduction

Solar irradiation holds immense potential as a sustainable and viable renewable energy source that can effectively meet a significant portion of the world's energy needs [1-4]. Solar cooling is an interesting concept as it involves the conversion of solar heat into cold or refrigeration, allowing cold to be produced from something warm [5-7]. Absorption refrigeration systems are considered to be a very favorable solar cooling technology [8,9]. These systems make use of environmentally friendly working fluids that do not contribute to global warming or ozone depletion. Moreover, they have a longer lifespan and require less maintenance [10]. Numerous studies have examined the use and research of absorption chillers in various academic papers. Within this area of study, Bellos et al. [11] conducted a study on the thermodynamic performance of an absorption chiller using LiBr-$H_2O$ incorporating four solar collectors. A cost analysis was conducted taking into account the costs associated with the collectors and the storage tank. The parabolic trough collector gave the highest exergy efficiency, which was measured at 5.504%. However, the evacuated tube collector was the best choice from an economic point of view. Liang et al. [12] evaluated a novel combined double ejector-absorption system using ammonia/salt working pairs. The numerical method was used to thoroughly examine the thermodynamic performance of the absorption refrigeration system. Gharir and Farshi [13] conducted an energy, exergy, and thermoeconomic evaluation of a newly proposed refrigeration cycle incorporating a double ejector and two flash tanks. The outcomes of the study were subsequently contrasted with those of a previously introduced absorption refrigeration cycle that operates with three pressure levels. Both systems utilize $NH_3$-$H_2O$ as the working fluid. The results indicated a significant improvement in both the coefficient of performance (COP) and COP-exe of the

1,3 Department of Mechanical Engineering, Bandar Anzali Branch, Islamic Azad University, Bandar Anzali, Iran. Email:rabiei_remm@yahoo.com, ad.kazemi@iau.ac.ir

**2* Corresponding Author:** Department of Mechanical Engineering, Lahijan Branch, Islamic Azad University, Lahijan, Iran. Email:Borji.mehdi@iau.ac.ir

***Received: 2024.09.25; Accepted: 2024.10.15***

proposed cycle when compared to the base cycle.

In this research, two different configurations of solar absorption refrigeration systems including single effect absorption and combined ejector-absorption refrigeration systems with flat plate solar collector and using three different working pairs: $NH_3$-$H_2O$, $NH_3$-$LiNO_3$ and $NH_3$-NaSCN were compared, investigated and analyzed from the viewpoints of energy, exergy and exergoeconomic. A review of the literature to date has shown that the previous researches conducted on this topic had many shortcomings and their study resulted in many ambiguities in understanding and no comprehensive and complete study has yet been carried out on the combined solar ejector-absorption refrigeration cycle using the liquid-vapor ejector at the entrance of the absorber and comparing and investigating its exergy and exergoeconomic performance using three working fluids based on ammonia with the solar single effect absorption cycle. Therefore, in this study we try to fill this research gap and we want to make a thorough analysis and study of the economic results, as well as evaluate the impact of different parameters on the solar collector area and other solar and economic parameters using three different working pairs, and finally conclude which of the studied working pairs has a better impact on the performance of the studied cycles. In addition, it is observed that $LiNO_3$and NaSCN are types of salts that have a crystalline arrangement in their solid form. When ammonia is used as a solvent for these salts, there is a specific temperature for each salt concentration at which the salt becomes solid. Preventing crystallization is therefore critical to absorption system design and operation. However, the absence of crystallization phenomena in ammonia-water systems can be considered an advantageous aspect.

## 2. Description of system configurations

Figure 1 demonstrates the single effect solar absorption refrigeration system, which consists of three main parts: the flat plate solar collector, the storage tank and the absorption cycle. The solar collector receives cold water at a temperature of $T_{20}$ from the lower layer of the storage tank and heats it; the collector then delivers hot water with a temperature of $T_{19}$ to the upper part of the storage tank. On the other side of the tank, water with the temperature of the heat source $(T_{11})$ leaves the upper part of the storage tank and enters the generator of the absorption system. This water, which gives heat to its countercurrent flow in the generator, decreases in temperature and enters the lower part of the tank with temperature $T_{12}$, until it enters the collector again and increase in temperature.

In the absorption cycle, the strong solution is discharged from the absorber (4) and pumped (5) to the solution heat exchanger where it is heated by the weak solution coming from the generator. The strong solution enters the generator (6) where the ammonia (refrigerant in each of these three working pairs) is extracted from the solution. The ammonia vapor leaves the generator (10) and condenses in the condenser.

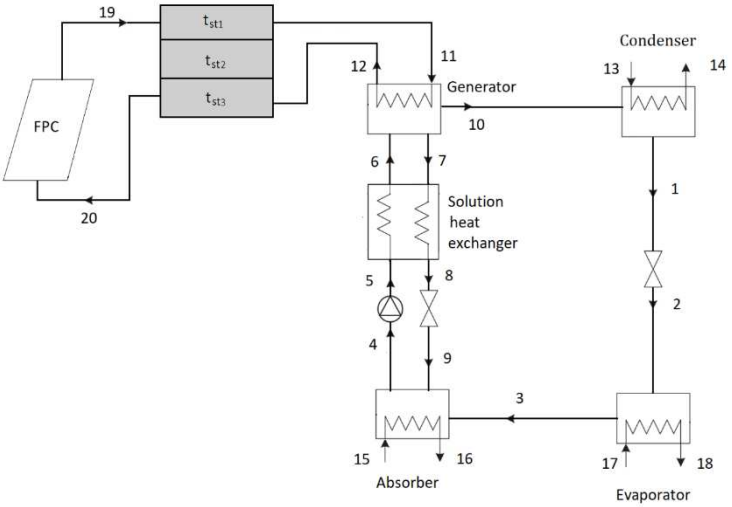


**Fig. 1.**Schematic diagram of solar single effect absorption refrigeration system

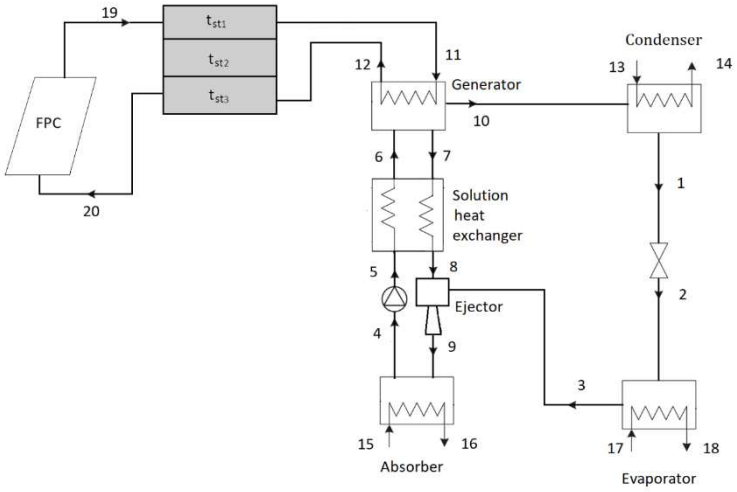


**Fig. 2.**Schematic diagram of combined solar ejector-absorption refrigeration system

The high-pressure liquid ammonia (refrigerant) passes through the throttling valve (1), which reduces its pressure to the lower pressure. The ammonia then enters the evaporator at low pressure where it evaporates and produces cooling (2). Finally, the ammonia vapor is absorbed by the absorber (3) and the cycle is repeated. The weak solution returns to the absorber via the solution heat

exchanger (7-8) and reduces its pressure via the solution expansion valve (8-9). The single effect absorption refrigeration cycle therefore operates with only two pressure levels: high pressure in the generator and condenser, and low pressure in the absorber and evaporator. If no pressure loss is considered between the generator and the condenser, their pressures will be equal.

The combined ejector-absorption refrigeration cycle (Fig. 2) differs from the single-effect absorption refrigeration cycle in that its absorber pressure is not equal to the evaporator pressure. Therefore, this combined cycle operates at three pressure levels. The generator at high pressure, the evaporator at low pressure and the absorber at an intermediate pressure. As shown in Figure 2, the solution expansion valve is replaced by the liquid-vapor ejector located at the absorber inlet (8-9). In this state, the weak solution enters the ejector at high pressure (the primary flow of the ejector) (8) and the low-pressure refrigerant vapor is drawn into the ejector from the evaporator (the secondary flow) (3). The ejector discharges the mixed stream into the absorber at intermediate pressure (9). As a result, the pressure in the absorber is increased relative to the pressure in the evaporator.

## 3. Mathematical modeling

**Table 1.**Input values of the systems [11,14,15]

| Parameter | Value |
|---|---|
| $T_{generator}$ | 85℃ |
| $T_{condenser} = T_{absorber}$ | 35℃ |
| $T_{evaporator}$ | 0℃ |
| $\varepsilon_{Solution\ heat\ exchanger}$ | 80% |
| $\eta_{Pump}$ | 95% |
| $\eta_{Nozzle}$ | 85% |
| $\eta_{Mixing}$ | 90% |
| $\eta_{Diffuser}$ | 80% |
| $D_{Diffuser}$ | 0.15 m |
| $G_{Tilted}$ | 800 $Wm^{-2}$ |

By modeling the two chillers in the engineering equation solver (EES), the energy, exergy, and exergy-economic studies of the configurations are performed. In the first step of simulating the two solar-driven chillers, some simplifying assumptions need to be made. These assumptions are outlined below [11,16,17]:

●Systems operate in steady state conditions.

● Frictional pressure losses in both heat exchangers and connecting pipework are assumed to be negligible.

● All throttle valves operate under adiabatic condition, resulting in constant enthalpy processes.

● The refrigerant leaves the evaporator and condenser as saturated vapor and liquid respectively.

● All systems are simulated and analyzed with a constant cooling capacity of $\dot{Q}_{evaporator}$=300 KW.

● The heat source temperature $(T_{11})$ is set to $T_{11} = T_{generator} + 10$ and the hot flow after the generator $(T_{12})$ is set to $T_{12} = T_{generator} + 5$.

● The reference environmental condition is set at a temperature of 25℃ and a pressure of 100 Kpa.

### 3.1 Analysis of the liquid ejector

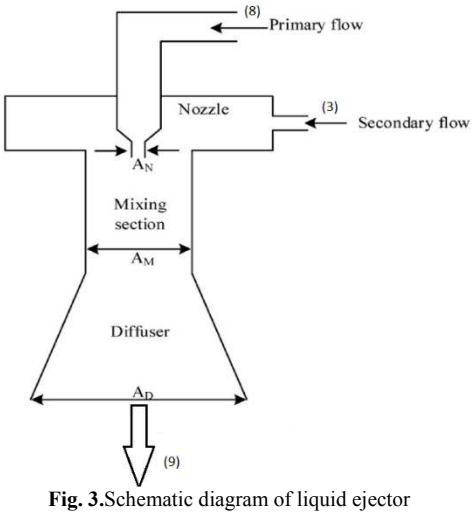


**Fig. 3.**Schematic diagram of liquid ejector

Figure 3 shows a schematic diagram of the liquid ejector. As shown, the ejector consists of three parts: the nozzle, the mixing chamber and the diffuser. As mentioned earlier, the weak solution leaving the heat exchanger (8) passes through a nozzle and mixes with the evaporated refrigerant (3) in the mixing tube of the ejector. The mixture leaves the diffuser at absorber pressure (9). In this study, a one-dimensional model is used based on the basic principles presented by Chen [18]. The simulation of the ejector was performed with certain assumptions, which can be summarized as follows [14,15,18]:

● There is no external heat transfer.

● The potential energy can be neglected.

● The primary and secondary fluids have low Mach numbers, so the flow is incompressible.

● The weak solution flows through the nozzle from the generator pressure (high pressure) to the evaporator

pressure (low pressure).

- After complete mixing at the outlet of the mixing section, all flow characteristics are uniform.
- The mixing and diffuser chambers do not involve any absorption process.
- The kinetic energies of the primary and secondary fluids are not considered.

The efficiencies and governing equations for the analysis of the liquid ejector in each section are given in Tables 1 and 2, respectively. Note that the unit of pressure used in Table 2 is Pa. In addition, the diameter of the diffuser does not significantly affect the performance of the ejector. As shown in Table 1, a diameter of 0.15 m was chosen for this section.

**Table 2.**Governing equations of the liquid ejector [14,15,19]

| Section | Equations | |
|---|---|---|
| Nozzle | $V_{N=}\left(\eta_N.2.\frac{1000(P_{con}-P_{eva})}{\rho_8}\right)^{0.5}$ | (1) |
| | $\rho_8 = \mathrm{f}\,(T_8,X_8)$ | (2) |
| | $A_N = \pi.\frac{D_N^2}{4}$ | (3) |
| | $A_N = \frac{\dot{m}_7}{\rho_8.V_N}$ | (4) |
| Mixing section | $V_M = \frac{\dot{m}_1+\dot{m}_7}{A_M.\rho_M}$ | (5) |
| | $A_M = \pi.\frac{D_M^2}{4}$ | (6) |
| | $\rho_M = \frac{\dot{m}_1+\dot{m}_7}{\frac{\dot{m}_1}{\rho_3}+\frac{\dot{m}_7}{\rho_8}}$ | (7) |
| | $P_{M=}P_{eva} + \eta_M.\frac{\dot{m}_7.V_N-(\dot{m}_7+\dot{m}_1).V_M}{A_M.1000}$ | (8) |
| Diffuser | $P_D = P_M + \frac{0.5.\rho_M.(V_M^2-V_D^2).\eta_D}{1000}$ | (9) |
| | $P_D = P_{abs}$ | (10) |
| | $V_D = \frac{(\dot{m}_7+\dot{m}_1)}{\rho_M.A_D}$ | (11) |
| | $A_D = \pi.\frac{D_D^2}{4}$ | (12) |
| | $\dot{m}_7.h_8 + \dot{m}_3.h_3 = \dot{m}_7.h_{9s} + \dot{m}_3.h_{9r}$ | (13) |

### 3.2Thermodynamic analysis

A coefficient of performance (COP) can be calculated from the first law analysis of the absorption system as follows:

$$COP = \frac{\dot{Q}_{eva}}{\dot{Q}_{gen}+\dot{W}_{pump}} \quad (14)$$

The exergetic efficiency of the system refers to the ratio of the desired output energy to the total input exergy of the system. It is calculated as follows:

$$\eta_{\prod} = \frac{-\dot{Q}_{eva}\left(1-\frac{T_0}{T_{cold}}\right)}{\dot{Q}_{gen}\left(1-\frac{T_0}{T_{hot}}\right)+\dot{W}_{pump}} \times 100 \quad (15)$$

The ratio of the absorber pressure (intermediate pressure) to the evaporator pressure (low pressure) is defined as the ejector pressure ratio:

$$Pr_{Ejector} = \frac{P_{abs}}{P_3} \quad (16)$$

The thermal efficiency of the flat plate collector is given by equation (17):

$$\eta_{col=0.75-5.\left(\frac{T_{Col,in}-T_0}{G_{Tilted}}\right)} \quad (17)$$

The total COP of the solar absorption cooling systems can be calculated as the solar coefficient of performance by use of equation (18):

$$SCOP = \frac{\dot{Q}_{eva}}{A_{col}.G_{Tilted}} \quad (18)$$

The solar exergetic efficiency of a solar cooling system is calculated in the following way:

$$\eta_{ex,solar} = \frac{-\dot{Q}_{eva}\left(1-\frac{T_0}{T_{cold}}\right)}{A_{col}.G_{Tilted}.\left[1-\frac{4}{3}.\left(\frac{T_0}{T_{sun}}\right)+\frac{1}{3}.\left(\frac{T_0}{T_{sun}}\right)^4\right]} \times 100 \quad (19)$$

The temperature of the sun $(T_{sun})$ in the above equation is 4350 K.

### 3.3Exergoeconomic analysis

Exergoeconomic analysis is based on the combination of the second law of thermodynamics and economic principles. In this study specific exergy costing (SPECO) approach is used for exergoeconomic analysis of the considered cycles. This approach includes the following steps: (1) the identification of the exergy flows, (2) the definition of fuel and product for each component of the system and (3) the development of the cost flow rate balance equations [20].

For each component of the cycles, the cost flow rate balance equation is expressed as:

$$c_Q \dot{E}x_Q + \sum c_{in}\dot{E}x_{in} + \dot{Z} = \sum c_{out}\dot{E}x_{out} + c_w\dot{W} \quad (20)$$

The capital cost of each component $(Z_k)$ is converted to a cost rate $(\dot{Z}_k)$ as follows [21]:

$$\dot{Z}_k = \frac{Z_k.CRF.\varphi}{N} \quad (21)$$

Where N is the annual runtime of the system, $\varphi$ is the maintenance factor (1.06), and CRF is the capital recovery factor, which can be expressed as [21]:

$$CRF = \frac{i(1+i)^n}{(1+i)^n-1} \quad (22)$$

Here, $i$ is the interest rate (10%) and $n$ is the lifetime of the system in years (20 years).

The purchase costs of the components are provided in Table 3.

**Table 3.**Purchase cost relations [22-26]

| Component | Relation |
|---|---|
| Solar collector | $Z_{FPC} = 235\ A_{Col}$ |
| Storage tank for every 400 L of storage tank capacity | $Z_{st} = 1380 \times V_{st} \times 0.4$ |
| Generator | $Z_{gen} = Z_{R,gen}\left(\frac{A_{gen}}{A_R}\right)^{0.6}, Z_{R,gen} = 17500\ \$, A_R = 100\ m^2$ |
| Solution heat exchanger | $Z_{SHX} = Z_{R,SHX}\left(\frac{A_{SHX}}{A_R}\right)^{0.6}, Z_{R,SHX} = 12000\ \$, A_R = 100\ m^2$ |
| Evaporator | $Z_{eva} = Z_{R,eva}\left(\frac{A_{eva}}{A_R}\right)^{0.6}, Z_{R,eva} = 16000\ \$, A_R = 100\ m^2$ |
| Condenser | $Z_{con} = Z_{R,con}\left(\frac{A_{con}}{A_R}\right)^{0.6}, Z_{R,con} = 8000\ \$, A_R = 100\ m^2$ |
| Absorber | $Z_{abs} = Z_{R,abs}\left(\frac{A_{abs}}{A_R}\right)^{0.6}, Z_{R,abs} = 16500\ \$, A_R = 100\ m^2$ |
| pump | $Z_P = Z_{R,P}\left(\frac{\dot{W}_P}{\dot{W}_{R,P}}\right)^{0.26}\left(\frac{1-\eta_P}{\eta_P}\right)^{0.5}, Z_{R,P} = 2100\ \$, \dot{W}_{R,P} = 10\ KW$ |
| Ejector | $Z_{\text{Ejector}} = 1000 \times 16.14 \times 0.989 \times \dot{m}_8\left(\frac{T_8}{0.1\ P_8}\right)^{0.05} \times (0.1\ P_{abs})^{-0.75}$ |

All cost data used in an economic analysis in different years must be adjusted to the same reference year using of the following relationship [21].

$$Cost\ at\ the\ reference\ year = original\ cost \times \left(\frac{cost\ index\ for\ the\ reference\ year}{cost\ index\ for\ the\ year\ when\ the\ original}\right) \quad (23)$$

The Marshall and Swift equipment cost index is used in this study for the updating of all costs to the year 2021 [27].

The exergy-economic performance of the systems is evaluated by calculating the total cost rate and the unit cost of cooling as the equations follow:

$$\dot{C}_{tot} = \dot{Z}_{tot} + \dot{C}_{Destruction,tot} \quad (24)$$

$$C_{cooling} = C_{18} (25)$$

## 4. Results and discussion

An exergy and exergoeconomic analysis are performed to compare the performance of solar single-effect absorption and combined solar ejector-absorption refrigeration cycles using $NH_3$-$H_2O$, $NH_3$-$LiNO_3$, and $NH_3$-NaSCN as working fluids. This analysis is carried out using a computer program coded in the EES. In order to analyze absorption refrigeration cycles, it is necessary to consider the thermophysical properties of the working fluids. The properties of the $NH_3$-$H_2O$ solution are used by the data provided in EES software library [28]. For $NH_3$-$LiNO_3$and $NH_3$-NaSCN systems, vapor pressure and density data are taken from Infante Ferreira [29], and the enthalpy and entropy data are taken from Farshi et al. [17].

To validate the modelling, the results of the solar ammonia-water absorption refrigeration cycle with identical input parameters were compared with the reference results [30] in Table 4.

**Table 4.**Comparison of the results of the present analysis with those of the reference [30]

| | Present analysis | Reference [30] |
|---|---|---|
| $\dot{Q}_{Gen}(KW)$ | 17.03 | 16.77 |
| $\dot{Q}_{Con}(KW)$ | 11.45 | 11.43 |
| $\dot{Q}_{Abs}(KW)$ | 15.63 | 15.33 |
| $\dot{Q}_{SHX}(KW)$ | 6.76 | 6.53 |
| COP | 0.585 | 0.60 |

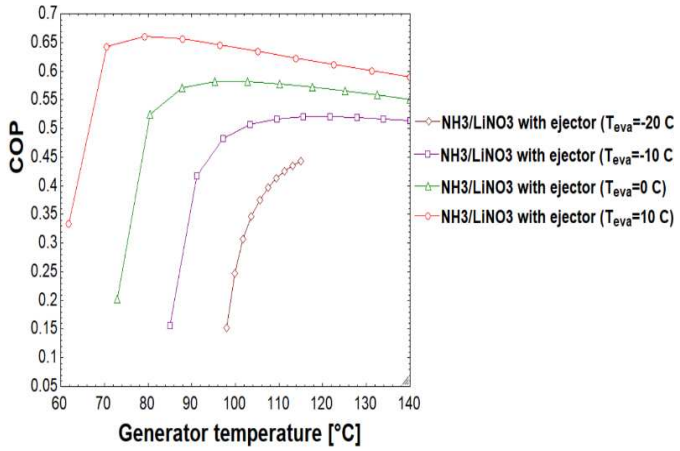


**Fig. 4.**COP verification of the combined ejector-absorption refrigeration cycle along with $NH_3$-$LiNO_3$ with those of the reference [14]

In addition, the COP of the combined ejector-absorption refrigeration cycle using NH3-LiNO3 as the working fluid has been compared with those of the reference [14] and illustrated in Figure 4. As can be seen, there is a good agreement between the obtained results and those of the mentioned references.

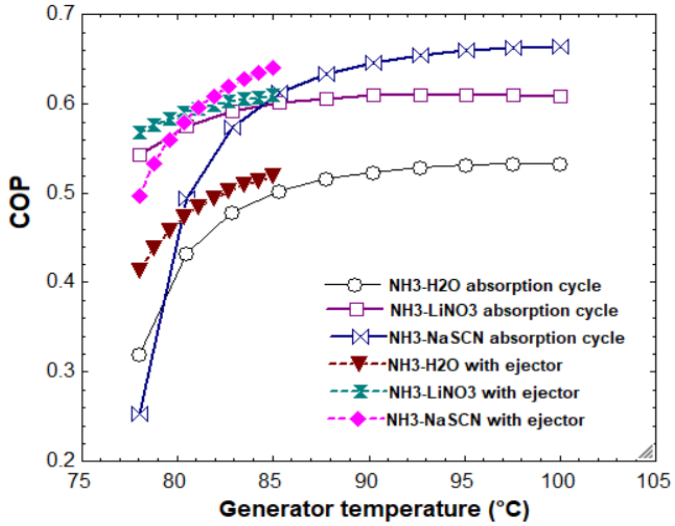


**Fig. 5.**Comparison of COP changes of solar absorption refrigeration cycles with increasing generator temperature using different working fluids based on ammonia

Figure 5 clearly shows that from the generator temperature of 85 ℃, there is an increase in the coefficient of performance in the simple absorption cycle with $NH_3$-NaSCN as the working fluid. In the combined ejector-absorption cycle, by increasing the ejector pressure ratio, an increase in the COP of the combined ejector-absorption cycle is observed compared to the simple absorption cycle, which is noticeable in the combined ejector cycle with $NH_3$-$H_2O$ and $NH_3$-NaSCN. In the combined ejector cycle with $NH_3$-NaSCN, from the generator temperature of 83 ℃, an increase in COP can be seen compared to this combined cycle with two other working fluids.

As can be seen in Figure 6, the simple absorption cycle with $NH_3$-NaSCN shows an increase in exergy efficiency compared to the simple absorption cycle with $NH_3$-$H_2O$ and $NH_3$-$LiNO_3$ from the generator temperature of 87 ℃ onwards. In addition, the simple absorption cycle with $NH_3$-$LiNO_3$ shows an increase in exergy efficiency at lower generator temperatures (up to 85 ℃). In a combined ejector-absorption refrigeration cycle with three different working fluids, it is observed that the exergy efficiency of the combined ejector cycle improves as the generator temperature increases to 82 ℃ when using $NH_3$-$LiNO_3$ as the working fluid. Similarly, an increase in the exergy efficiency of the combined ejector cycle with $NH_3$-NaSCN is observed as the generator temperature reaches between 83℃ and 85℃. As the ejector pressure ratio increases, the combined ejector-absorption cycle with $NH_3$-NaSCN has the highest increase in exergy efficiency compared to the simple absorption cycle with $NH_3$-NaSCN. Similarly, the combined ejector-absorption cycle with $NH_3$-$LiNO_3$ has the lowest increase in exergy efficiency compared to the simple absorption cycle with $NH_3$-$LiNO_3$ as the working fluid.

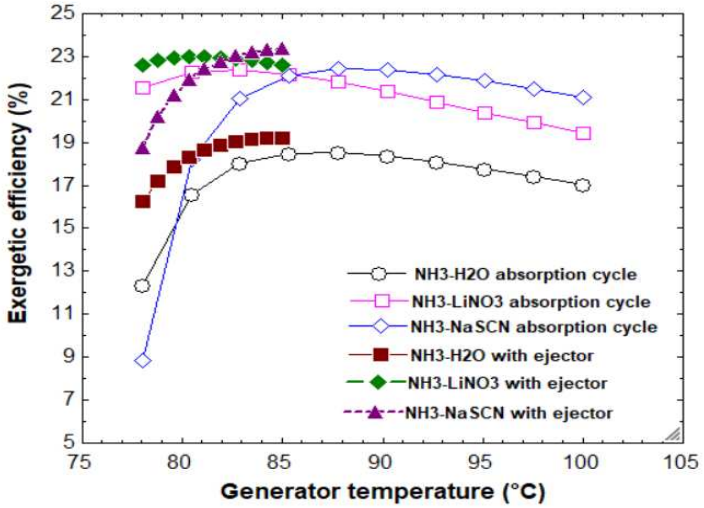


**Fig. 6.**Comparison of the effect of the generator temperature increase on the variation of the exergy efficiency of solar absorption cycles using different working fluids based on ammonia

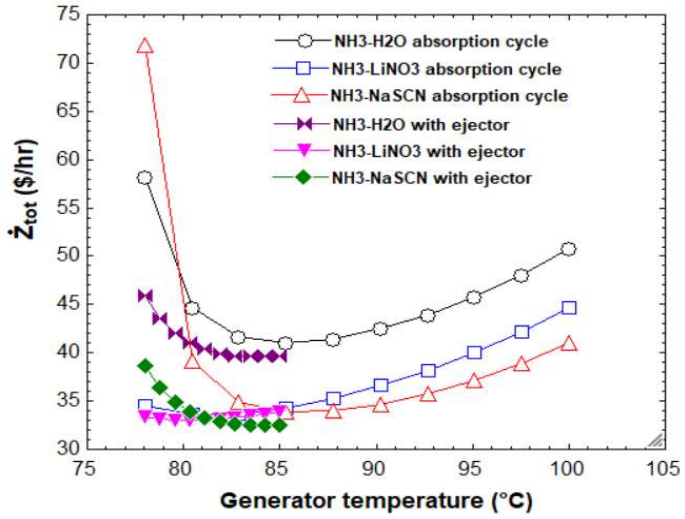


**Fig. 7.**Comparison of the effect of generator temperature change on the total investment cost rate of the systems studied, using different working fluids based on ammonia

The information presented in Figure 7 illustrates that in the simple absorption cycle with $NH_3$-NaSCN, the total investment cost rate decreases from a generator temperature of 86 ℃ compared to the simple absorption cycle with two other working fluids. At low generator temperatures (up to 85 ℃), a reduction in the total investment cost rate of the simple absorption cycle with $NH_3$-$LiNO_3$ is observed. By increasing the ejector pressure ratio, the total investment cost rate of the combined ejector-absorption cycle with $NH_3$-$H_2O$ and $NH_3$-NaSCN decreases compared to the simple absorption cycle with the same working fluids.In the combined ejector-absorption cycle and among the three working fluids mentioned, a decrease in the total investment cost rate can be seen from 82℃ to 85℃ when using the combined ejector cycle with $NH_3$-NaSCN as the working fluid. Regarding the trend of changes in the total investment cost rate, in the cycles studied, as the generator temperature increases, in the simple absorption cycles with three different working fluids and also in the combined ejector cycle with $NH_3$-$LiNO_3$, the total investment cost rate initially reaches a minimum value and then follows an increasing trend. In the combined ejector cycle with $NH_3$-$H_2O$ and $NH_3$-NaSCN, the total investment cost rate initially decreases and then stabilizes as the generator temperature increases. The determining factor in all these overall trend variations is the trend of changes in the solar collector and storage tank investment cost rate, which has a dominant effect on the total investment cost rate.

As shown in Figures 8 and 9, the total cost rate of exergy destruction and the total cost rate in the combined ejector-absorption cycle decrease as the ejector pressure ratio increases compared to the simple absorption cycle. This decrease is noticeable in the combined ejector-absorption cycle with $NH_3$-$H_2O$ and $NH_3$-NaSCN. The total cost rate of exergy destruction and the total cost rate in the combined ejector-absorption cycle with $NH_3$-$LiNO_3$ are lower compared to the combined ejector cycle with $NH_3$-$H_2O$ and $NH_3$-NaSCN from a generator temperature of 78 ℃ to 82℃. Also, in the combined ejector cycle with $NH_3$-NaSCN from a generator temperature of 83 ℃ to 85℃, the total cost rate of exergy destruction and the total cost rate are lower compared to the combined ejector cycle with $NH_3$-$H_2O$ and $NH_3$-$LiNO_3$. In the simple absorption cycle with $NH_3$-NaSCN, the total cost rate of exergy destruction and the total cost rate decrease from a generator temperature of 86 ℃ compared to the simple absorption cycle with $NH_3$-$H_2O$ and $NH_3$-$LiNO_3$.According to equation (24), the total cost rate of the system is equal to the sum of the total investment cost rate and the cost rate of exergy destruction. As a result, the increase of the generator temperature and its effects on the total investment cost rate and the total exergy destruction cost rate of the different components of the studied cycles cause the changes observed in Figure 9 for the total cost rate of the systems.

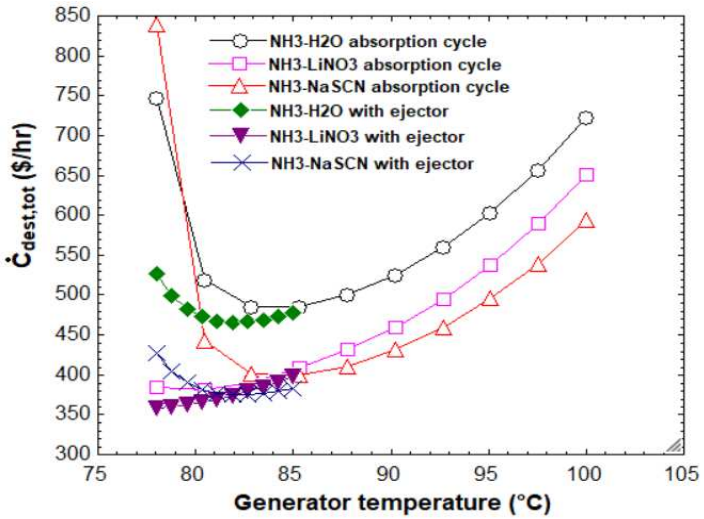


**Fig. 8.**Comparison of the effect of the generator temperature change on the total cost rate of exergy destruction of the systems being studied, with different working fluids on the basis of ammonia

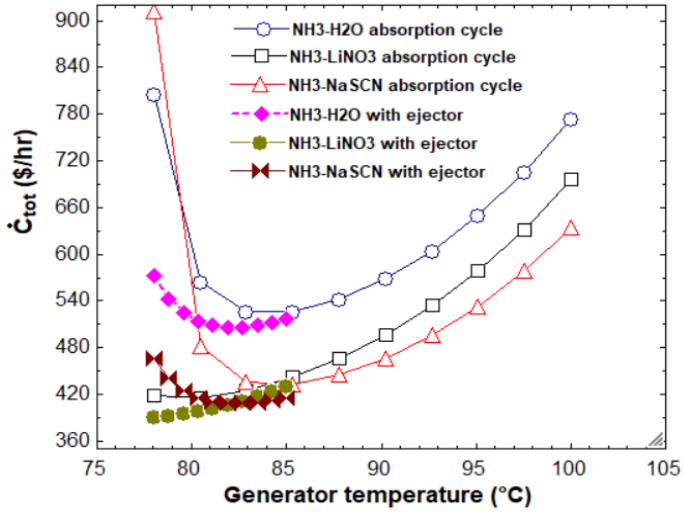


**Fig. 9.**comparison ofthe effect of generator temperature change on the total cost rate of systems being examined, using different working fluids based on ammonia

By solving a set of exergy-economic equations for the system under study, the unit cost of cooling production is obtained.As seen in Figure 10, the minimum value of the unit cost of cooling production is related to the simple and combined absorption cycles with $NH_3$-$LiNO_3$.

As depicted in Figures 11 and 12, in the simple absorption cycle with $NH_3$-NaSCN, the solar coefficient of performance and the solar exergetic efficiency increase compared to the simple absorption cycle with $NH_3$-$H_2O$ and $NH_3$-$LiNO_3$, starting from a generator temperature of 85℃.

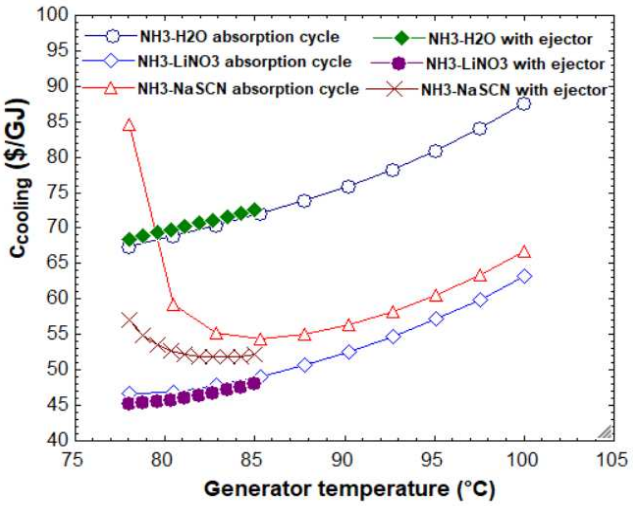


**Fig. 10.**Comparing the effect of changing the generator temperature on the unit cost of cooling production of the systems being studied using different working fluids based on ammonia

With this increase, as observed in Figure 13, in the simple absorption cycle with $NH_3$-NaSCN, the area of the solar collector decreases from a temperature of 85℃ compared to the simple absorption cycle with the other two working fluids. Also, looking at Figures 11 and 12, with an increase in the ejector pressure ratio, we observe an increase in the solar coefficient of performance and solar exergetic efficiency in the combined ejector cycle with the three working fluids mentioned. This increase is particularly noticeable in the combined ejector cycle with $NH_3$-NaSCN. The opposite process occurs for the solar collector area in Figure 13.

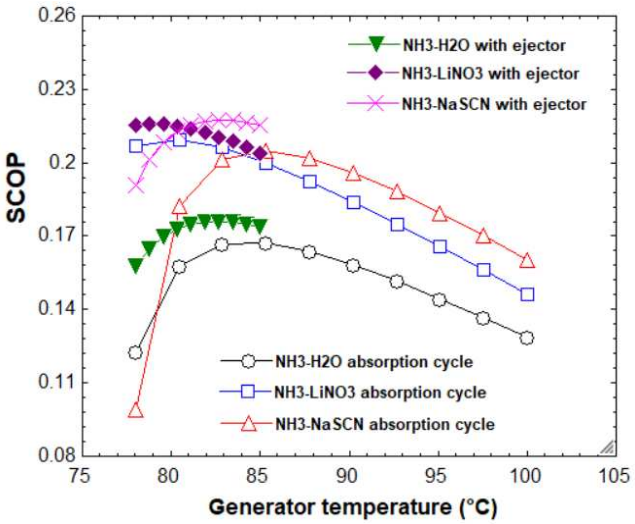


**Fig. 11.**Comparison of the effect of the generator temperature change on the solar coefficient of performance of the systems studied using different working fluids based on ammonia

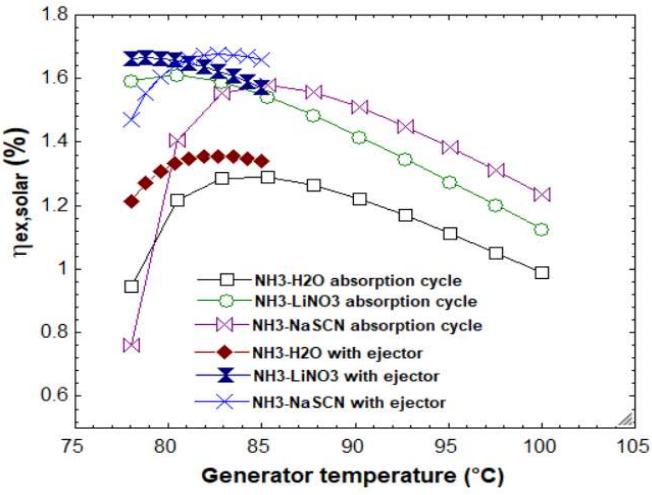


**Fig. 12.**Comparison of the effect of generator temperature variation on the solar exergy efficiency of systems studied using different working fluids based on ammonia

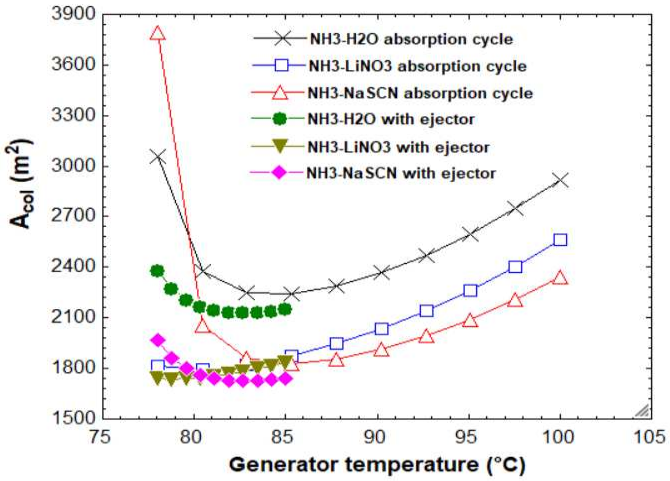


**Fig. 13.**Comparison of the effect of the generator temperature change on the collector area of the systems studied using different working fluids based on ammonia

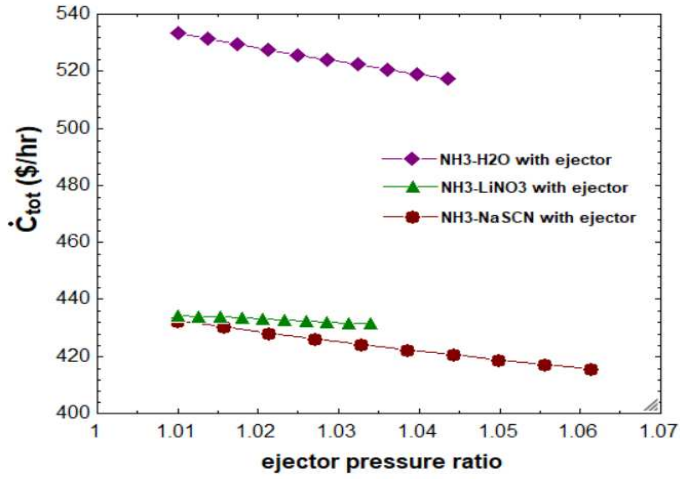


**Fig. 14.**The effect of increasing the ejector pressure ratio on total cost rate in the combined ejector-absorption cycle with different working fluids based on ammonia

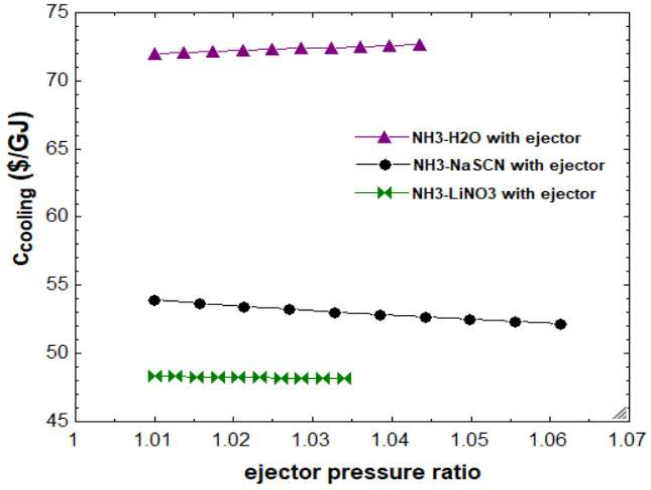


**Fig. 15.**The effect of increasing the ejector pressure ratio on the unit cost of cooling production in the combined ejector-absorption cycle with different working fluids based on ammonia

Figures 14 and 15 show that as the ejector pressure ratio increases, the lowest total cost rate is achieved in the combined ejector-absorption cycle with $NH_3$-NaSCN, and the lowest unit cost of cooling production is observed in the combined ejector-absorption cycle with $NH_3$-$LiNO_3$ as the working fluid.

As mentioned in section 1, the absorbents used in this study are lithium nitrate and sodium thiocyanate, which are salts. Therefore, the risk of crystallization should be avoided in these cycles. The point where the solution enters the absorber, which is state 9 in these cycles studied, has the highest concentration of salt and the lowest temperature. This makes it the most likely place for crystallization to occur. To study this phenomenon in the cycles studied, the temperature and concentration of state 9 are determined for each operating condition. These values are then compared with the concentration of crystallization at that temperature. Infante Ferreira [29] correlated the experimental solubility data and provided the equations of the crystallization line for the $NH_3$-$LiNO_3$ and $NH_3$-NaSCN solutions used in this study. In the figures presented in this study, according to the temperature range of the generator, which is shown up to a temperature of 100 ℃, crystallization does not occur. Based on the investigations carried out in the present study and considering the equations related to Ferreira [29], crystallization occurs from a generator temperature of 145℃ and above for the absorption cycle with $NH_3$-$LiNO_3$ and from 118 ℃ and above for the absorption cycle with $NH_3$-NaSCN. In the combined ejector cycle and considering the geometry of this type of ejector, the range of generator temperatures at which the combined ejector cycle can operate without crystallization is limited compared to the simple absorption cycle. Also, the ammonia-sodium thiocyanate cycle cannot operate at evaporator temperatures below -10 ℃ due to the possibility of crystallization [29].

## 5. Conclusions

In this research, two different solar absorption cycles have been investigated, including the combined solar ejector-absorption cycle and the simple solar absorption cycle using ammonia-water, ammonia-lithium nitrate, and ammonia-sodium thiocyanate solutions as working fluids. The systems are simulated, analyzed and compared in terms of energy, exergy, and exergoeconomic using flat plate solar collector and storage tank. Parametric analysis was performed on these systems. This study also addressed the research gaps and scientific ambiguities related to the economic factors and the use of solar energy as a driving

source for the combined ejector-absorption cycle with the use of liquid-vapor ejector located at the absorber inlet. Finally, it has been studied which of the mentioned working fluids perform well in terms of exergy and exergoeconomic in the cycles studied. The simulation results show that:

● The parametric energy and exergy analysis shows that increasing the generator temperature in the simple absorption cycle and the combined ejector-absorption cycle with $NH_3$-NaSCN working fluid leads to improvements in the coefficientof performance, exergy efficiency, solar coefficient of performance, and solar exergetic efficiency of these cycles, especially at higher generator temperatures, compared to these cycles with $NH_3$-$H_2O$ and $NH_3$-$LiNO_3$ working fluids.

● The analysis of the results of the parametric studies from the exergoeconomic point of view shows that with an increase of the generator temperature, in both the simple absorption and the combined ejector-absorption cycles with $NH_3$-NaSCN as working fluid, there is a reduction of the investment cost rate, cost rate of exergy destruction, total cost rate and, consequently, an improvement of the economic performance of these cycles, especially at higher generator temperatures, compared to the cycles studied with $NH_3$-$H_2O$ and $NH_3$-$LiNO_3$. Furthermore, the total cost rate and consequently the economic performance of the combined ejector cycle with $NH_3$-NaSCN are also reduced as the ejector pressure ratio increases.

●With the increase of the generator temperature in the simple absorption and combined ejector-absorption cycles, as well as with the increase of the ejector pressure ratio, a decrease and consequently an improvement of the unit cost of cooling production is observed in the studied absorption cycles using $NH_3$-$LiNO_3$.

● In the combined ejector-absorption cycle with $NH_3$-NaSCN, a decrease in the solar collector area is observed as the generator temperature and also the ejector pressure ratio increases in the cycles studied.

● In six cycles considered, the highest values of heat transfer rate, rate of exergy destruction, cost rate of exergy destruction and total cost rate are associated with the solar collector. Therefore, this component should receive more attention than other components from an exergoeconomic point of view. In addition, the cycles studied with the working fluid of $NH_3$-NaSCN show better performance in terms of exergy and exergoeconomic compared to these cycles with $NH_3$-$H_2O$ and $NH_3$-$LiNO_3$ working fluids.

● In the ammonia-sodium thiocyanate combined ejector cycle, which has the best performance among the cycles studied, the coefficient of performance, exergy efficiency, solar coefficient of performance and solar exergy efficiency are equal to 0.64,23.41%, 0.21 and 1.659%, respectively. Also, the total cost rate and the unit cost of cooling production in the mentioned cycle are equal to 415.7 $\frac{\$}{hr}$ and 52.15 $\frac{\$}{GJ}$, respectively.

● As a final conclusion, the cycles studied with $NH_3$-NaSCN working fluid show the best performance in terms of energy, exergy, and exergoeconomic aspects compared to these cycles with $NH_3$-$H_2O$ and $NH_3$-$LiNO_3$ working fluids (especially at higher generator temperatures). In terms of unit cost of cooling production, the cycles studied with $NH_3$-$LiNO_3$ show better performance compared to the other two working fluids.

**References**

[1] Mishra R.S and Singh Harwinder,*Detailed parametric analysis of solar driven supercritical CO2 based combined cycle for power generation, cooling and heating effect by vapor absorption refrigeration as a bottoming cycle*; Thermal Science and Engineering Progress,p. 397-410, 2018.

[2] Pourasl H, Vatankhah Barenji R and Khojastehnezhad V,*Solar energy status in the world: A comprehensive review;* Energy Reports,p. 3474-3493, 2023.

[3] Arroyo A, Basurto N, Casado-Vara R, Timiraos M and Calvo-Rolle J. *A Hybrid Intelligent Modeling approach for predicting the solar thermal panel energy production;* Neurocomputing,p. 126997, 2024.

[4] Buragohain S, Mohanty K and Mahanta P. *Experimental investigations of a 1 KW solar photovoltaic plant in standalone and grid mode at different loading conditions;* Sustainable Energy Technologies and Assessments,p. 100796, 2020.

[5] Bellos E, Chatzovoulos I and Tzivanidis C,*Yearly investigation of a solar-driven absorption refrigeration system with ammonia-water absorption pair;* Thermal Science and Engineering Progress,p. 100885, 2021.

[6] Yu X, Jiang S and Zhang S. *Energy, exergy, economic and environmental assessment of solar photovoltaic direct-drive refrigeration system forelectronic device cooling*; Renewable Energy,p. 119538, 2023.

[7] Mateo-Villanueva M and Echarri R,*Solar adsorption refrigeration system: Comparison between equilibrium, universal and transient model;* International Journal of Refrigeration,p. 23-33, 2024.

[8] Pataro I M.L, Gil J.D, Guzman J L, Berenguel M and Lemos J,*Hierarchical control based on a hybrid nonlinear predictive strategy for a solar-powered absorption machine facility;* Energy,p. 126964, 2023.

[9] Mendiburu AZ, Roberts JJ, Rodrigues LJ and Verma

SK,*Thermodynamic modelling for absorption refrigeration cycles powered by solar energy and a case study for Porto Alegre, Brazil*; Energy,p. 126457, 2023.

[10] Siddique MZ, Badar A W, Siddiqui M S, Butt F S, Saleem M, Mahmood K and Fazal I,*Performance analysis of double effect solar absorption cooling system with different schemes of hot/cold auxiliary integration and parallel-serial arrangement of solar field;* Energy,p.123299, 2022.

[11] Bellos E, Tzivanidis C and Antonopoulos KA. *Exergetic, energetic and financial evaluation of a solar driven absorption cooling system with various collector types;*Applied Thermal Engineering,p.749–59, 2016.

[12] Liang X, Zhou S, Deng J, He G and Cai D,*Thermodynamic analysis of a novel combined double ejector-absorption refrigeration system using ammonia/salt working pairs without mechanical pumps;* Energy,p. 185: 895-909, 2019.

[13] Dhahi Gharir A and Garousi Farshi L,*Proposal of a double ejector-two flash tank absorption refrigeration cycle: Energy, exergy and thermoeconomic evaluation;* Case Studies in Thermal Engineering,p. 103498, 2023.

[14] Garousi Farshi L, Mosaffa AH, Infante Ferreira CA and Rosen MA,*Thermodynamic analysis and comparison of combined ejector-absorption and single effect absorption refrigeration systems;* Applied Energy,p. 335-346, 2014.

[15] Kumar A and Modi A,*Thermodynamic analysis of novel ejector-assisted vapour absorption-resorption refrigeration systems;* Energy,p: 123154, 2022.

[16] Bellos E, Tzivanidis C and Antonopoulos K.A,*Exergetic and energetic comparison of LiCl-H2O and LiBr-H2O working pairs in a solar absorption cooling system;* Energy Conversion and Management,p. 453-461, 2016.

[17] Garousi Farshi L, Infante Ferreira CA, Seyed Mahmoudi SM and Rosen MA,*First and second law analysis of ammonia/salt absorption refrigeration systems;* International Journal of Refrigeration,p.111-21, 2014.

[18] Chen LT,*A new ejector-absorber cycle to improve the COP of an absorption refrigeration system;* Applied Energy,p. 37-51, 1988.

[19] Vereda C, Ventas R, Lecuona A and Venegas M,*Study of an ejector–absorption refrigeration cycle with an adaptable ejector nozzle for different working conditions;* Applied Energy,p.305–312, 2012.

[20] Shokati N and Khanahmadzadeh S, *The effect of different combinations of ammonia-water Rankine and absorption refrigeration cycles on the exergoeconomic performance of the cogeneration cycle;* Applied Thermal Engineering, p.1141-1160, 2018.

[21] Bejan, A. and Moran, M.J., 1996. Thermal Design and Optimization. Wiley. com.

[22] Ahmadi P, Dincer I and Marc A.R,*Multi-objective optimization of a novel solar-based multigeneration energy system*; Solar Energy,p. 576-591, 2014.

[23] Ahmadi Boyaghchi F, Mahmoodnezhad M and Sabeti V,*Exergoeconomic analysis and optimization of a solar driven dual-evaporator vapor compression-absorption cascade refrigeration system using water/CuO nanofluid;* Journal of Cleaner Production,p. 970-985, 2016.

[24] Misra R.D, Sahoo P.K, Sahoo S and Gupta A,*Thermoeconomic optimization of a single effect water/LiBr vapour absorption refrigeration system;* International Journal of Refrigeration,p. 158-169, 2003.

[25] Garousi Farshi L, Mahmoudi S, Rosen M, Yari M and Amidpour M,*Exergoeconomic analysis of double effect absorption refrigeration systems;* Energy Conversion and Management,p. 13-25, 2013.

[26] Bai H, Luo S, Zhao X, Zhao G and Yang G,*Comprehensive assessment of a green cogeneration system based on compressed air energy storage (CAES) and zeotropic mixtures;* Energy,p.124190, 2022.

[27] Economic indicators. Marshall & Swift Equipment Cost Index, Chemical Engineering, September 2021.

[28] Salehi S and Yari M,*Exergoeconomic assessment of two novel absorption-ejection heat pumps for the purposes of supermarkets simultaneous heating and refrigeration using $NaSCN/NH_3$, $LiNO_3/NH_3$ and $H_2O/NH_3$ as working pairs;* International Journal of Refrigeration,p.178-195, 2019.

[29] Infante Ferreira CA,*Thermodynamic and physical property data equations for ammonia-lithium nitrate and ammonia-sodium thiocyanate solutions;* Solar Energy,p. 231-236, 1984.

[30] Aman J, Ting D.S-K and Henshaw P,*Residential solar air conditioning: Energy and exergy analyses of an ammonia-water absorption cooling system;* Applied Thermal Engineering,p.424-432, 2014.